NUCLEAR RESONANCE SCATTERING OF CIRCULARLY POLARIZED SR

K. Szymański[a], D. Satuła[a], L. Dobrzyński[a,b] and B. Kalska[†c]

[a]Institute of Experimental Physics, University of Białystok
Lipowa 41, 15-424 Białystok, Poland
[b]The Sołtan Institute for Nuclear Studies
05-400 Otwock-Świerk, Poland
[c]Free University Berlin, Institute of Experimental Physics
Arnimalle 14, 114 195 Berlin, Germany

(Received April 7, 2004)

Results of the experiments with nuclear resonance scattering of synchrotron radiation aiming at construction of the circularly polarized beam suitable for nuclear hyperfine studies are reported. Si(4 0 0) single crystal slab, 100 μm thick, was used as a quarter wave plate. Observed twofold reduction of the intensity in proposed geometry is due to the Si crystal itself. Hyperfine interactions are used to probe polarization state of the synchrotron beam. Too large angular beam divergence did not allow for achieving full circular polarization of photons. Consequently, further experiments are proposed to overcame beam divergence problems. A number of calculations presented in the paper show that cheap and easily available Si plate can serve as an effective desired polarizer.

PACS numbers: 76.80.+y, 07.85.Qe, 75.25.+z

1. Introduction

Nuclear Resonance Scattering (NRS) [1,2] proved to be powerful tool in investigation of hyperfine structure of the Mössbauer nuclei. High degree of polarization of the synchrotron radiation is a property that can be helpful in enriching information about the hyperfine structure under study. Because a change of the initial polarisation state of the beam results in a change of the amplitudes of the interfering components, experimental determination of the orientation of hyperfine fields is possible. Many experiments have been performed so far with linearly polarized incident beams [3–5]. Other

[†] Present address: University of Białystok, Institute of Chemistry, Hurtowa 1 15-399 Białystok, Poland.

polarization states, particularly the circular ones, may, however, also be useful because the circularly polarized radiation is sensitive to the sign of the hyperfine magnetic field. We are thus interested in a device, which would easily change linear to circular polarization of highly monochromatized radiation for NRS experiments. The circular polarization of the resonant beam can be generated by insertion of the ^{57}Fe foil, magnetized parallel to the $\boldsymbol{k}$ vector of photon, as suggested in early paper of Frauenfelder [6]. However this leads to the beam polarization which is nonuniform across the useful energy range.

In order to transform linear to circular polarization one can use the Bragg scattering from a quarter plate. It was already demonstrated that single crystal Si plate, working in asymmetric Bragg geometry in the vicinity of Si(1 1 1) peak, serves as convenient quarter wave plate in transmission geometry [7,8]. The authors of the cited papers achieved circular polarization degree as high as 0.9. It was already noticed in [7] that the finite angular divergence of the incident beam causes smearing of the polarization states through the spread of the phase shift. Later on diamond (1 1 1) [9] and Si(3 3 3) [10] were used as a quarter wave plates.

The sophisticated monochromators dedicated for nuclear resonance studies monochromatize the 10^4 eV range synchrotron beam to 10^{-3} eV range [11]. However, in the typical stations horizontal beam divergence is much larger than the vertical one. As we will see this property makes some type of experiments not feasible. It is not clear how the polarization state of highly monochromatized resonant beam with relatively large horizontal divergence will be affected by transmission quarter wave plate, and whether the intensity reduction will not make NRS measurements impossible. This paper reports the results of using Si single crystals as the x-ray optical element causing a change of the linearly polarized beam of resonant radiation to the circularly polarized beam as indicated in [7–10]. The experiments with nuclear resonant scattering of circularly polarized radiation are not common and to our knowledge only the [12] report is published till now.

It follows from the Ref. [13], that the best condition for operation of the quarter wave plate is ensured when one maximizes the $\mathrm{Re}(\chi_K\chi_{-K})\sin 2\theta_\mathrm{B}$, where θ_B is Bragg angle and χ_K is the Fourier transform of the susceptibility. We have found that for Si crystal and 14.4 keV energy maximum of the $\mathrm{Re}(\chi_K\chi_{-K})\sin 2\theta_\mathrm{B}$ is achieved for Si(4 0 0) scattering planes. In order to determine polarization state of the beam, well-known hyperfine structure of the ^{57}Fe nucleus was used as a probe of the beam polarization. The experiment was performed in two steps: first, the ^{57}Fe foil was characterized with linearly polarized radiation. Then the quarter wave plate was inserted and the resonant scattering from the foil was used as a probe of the polarization state of the beam.

2. Idea of the experiment

The radiation used in the experiment is linearly polarized: $\boldsymbol{E}$ and $\boldsymbol{B}$ vectors of a photon with wavevector $\boldsymbol{k}$ are directed as in Fig. 1. Polycrystalline ^{57}Fe iron foil with the surface of the foil oriented perpendicularly to the $\boldsymbol{k}$ vector of photons is inserted into the beam. When the foil is fully

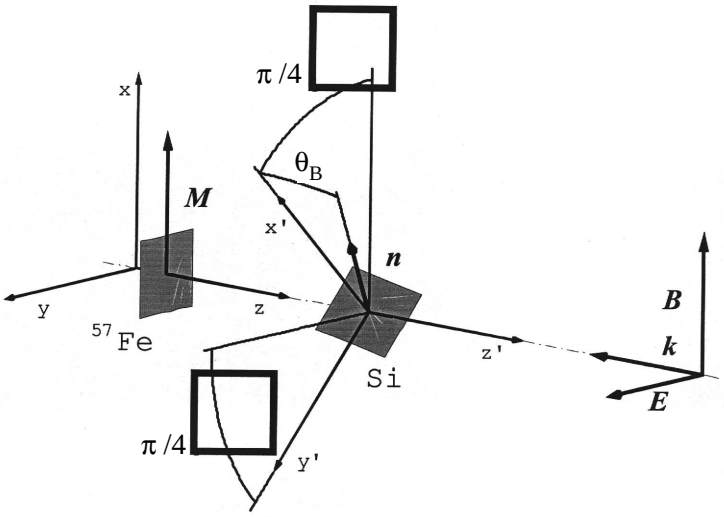


Fig. 1. Scheme of the experimental setup, and the coordination system used, see text.

magnetized perpendicular to the $\boldsymbol{E}$ vector (Fig. 1), one observes quantum beating pattern with a single frequency, see Fig. 2(a). The spectrum corresponds to the lines 2 and 5 of the Zeeman sextet in the energy domain. After rotating direction of magnetization by $\pi/2$ (magnetization parallel to the $\boldsymbol{E}$ vector) one expects to observe additional frequencies. The time beating corresponds to the lines 1,3,4,6 of the Zeeman sextet in energy domain [14], see Fig. 2(b). After insertion of ideal quarter wave plate, photons become circularly polarized and the time spectrum should not depend on the direction of magnetization in the plane. Simulated spectrum is shown in Fig. 2(c). For simplicity reasons all the spectra shown in Fig. 2 correspond to limiting case of thin absorber. In the case of thick absorber, shape of the spectrum is modulated by dynamical beats, predicted by theory of nuclear resonant scattering, see [15] for a review.

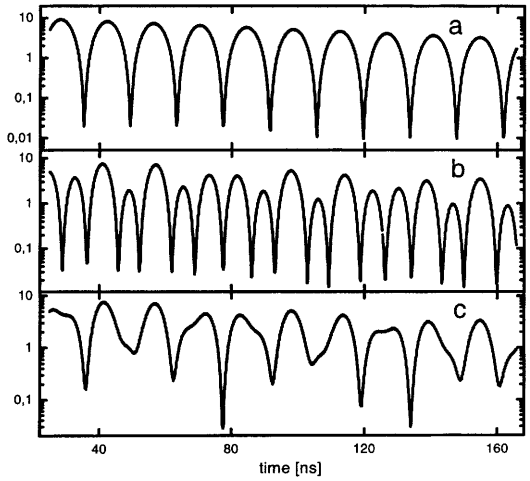


Fig. 2. Simulated spectra of the thin ^{57}Fe foil (a) magnetized perpendicularly to the $\boldsymbol{k}$ and $\boldsymbol{E}$ vectors of photon, measured with linearly polarized beam, (b) magnetized perpendicularly to the $\boldsymbol{k}$ and parallel to the $\boldsymbol{E}$, measured with linearly polarized beam, (c) magnetized perpendicularly to the $\boldsymbol{k}$, measured with circularly polarized beam.

3. Results

Commercial Si single crystals grown by Czochralski method (producer: Institute of Electronic Materials Technology, ITME, Warsaw), with the thickness of 100 μm were cut parallel to Si(1 0 0) planes and annealed for 1 h at 600° C to remove strains. Rocking curves of the Si plate were measured by neutron diffraction at MARIA reactor at Świerk, Poland, and compared with the rocking curves of almost perfect thick Si crystals. It was found that our crystal consists of mosaic blocks with relative orientation spread of the order of 100 μrad. Although this value is much larger than the Darwin width, one could hope that small linear size (about 0.5 mm) of the synchrotron beam used in our experiments will probe only a single block. Indeed, the width of the obtained transmission curves confirmed these expectations.

To insert the plate in the beam we used a holder having flat top surface at appropriate Bragg angle and a horizontal channel for 14.4 keV X rays. The Si sample was put on the top surface of the holder. The radiation was passing through the Si crystal and the channel in the holder. By this holder, mounted on the goniometer, we were able to scan the Si sample in the vicinity of Bragg angle and also to rotate the sample by $\pi/4$ along the $\boldsymbol{k}$ vector of radiation (see Fig. 1). ^{57}Fe foil was rolled and annealed for 2 h at

1173 K in order to recrystallize and remove strains. The thickness measured at different points of the foil varied from 10 to 14 μm. The foil was inserted between two poles of permanent Fe-Nd-B magnet. The cylindrical magnets produce field of about 0.203(1) T. The second derivative of the field along symmetry axis was measured to be 1.5(1) mT/mm^2.

The experiment was performed at BW4 station of DORIS ring at Hasylab, DESY. 2.7 m wiggler equipped with magnet of hybrid type produced X -ray radiation. Resonant photons were obtained after the scattering from the Si(4 2 2)×Si(12 2 2) channel cut nested monochromator [16]. The beam was collimated by four pairs of slits. Horizontal and vertical pairs of primary slits were separated by 17.2 meters from vertical and horizontal pairs of slits located close to the sample. The maximum slits opening was about 1.5 mm and the beam size was much smaller then the source size. All measurements were done at room temperature. Within vertical divergence of the beam no linear polarization changes are expected.

Initially the time spectra from the magnetized iron foil were measured. The results, presented in Fig. 3, clearly show beatings corresponding to σ and π polarizations of the transitions. Next, the foil was removed and the Si plate

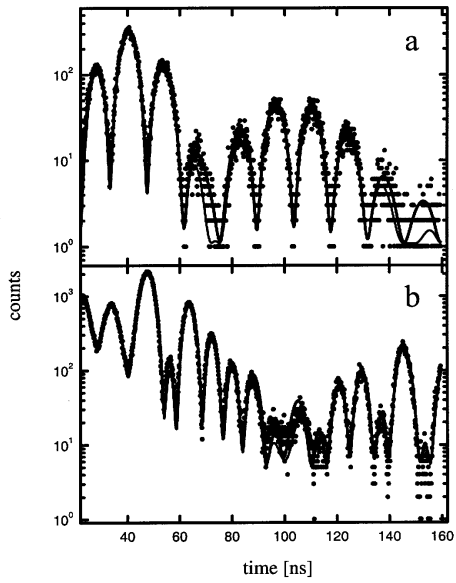


Fig. 3. NRS from ^{57}Fe foil in external magnetic field. The axis of the magnet is oriented (a) perpendicular (b) parallel to the $\boldsymbol{E}$ vector of photons at linear polarization state. Surface of the foil is oriented perpendicularly to the $\boldsymbol{k}$ vector of photons. Two solid lines on each graph correspond to the best fit. The thick lines correspond to the fit including distribution of the thickness parameter. Thin lines correspond to the single value of the thickness parameter.

was inserted at angle corresponding to Si(4 0 0) Bragg peak. The $\boldsymbol{n}$ vector, normal to the scattering planes (and normal to Si plate), lies at the direction $\pm\pi/4$ with respect to $\boldsymbol{E}$ and $\boldsymbol{B}$ vectors, respectively (see Fig. 1). Measured transmitted intensity with all slits opened (about 1.5 mm each) is shown in Fig. 4. Since the Bragg angle was not measured with high precision, zero position in Fig. 4 was set at the minimum of the transmission curve. After selecting an angular position of the plate (see one of the seven bars in Fig. 4),

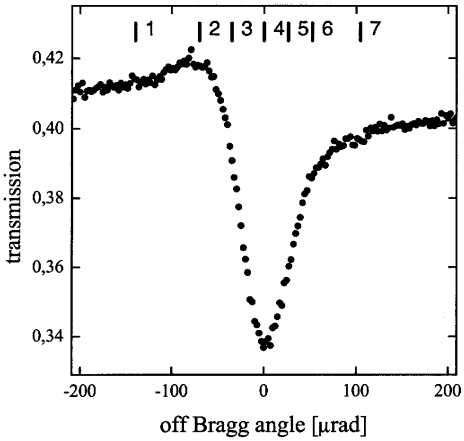


Fig. 4. Rocking curve of the transmitted intensity (Bragg geometry) in the vicinity of Si(4 0 0) Bragg peak. Horizontal scale was set to have 0 at the position of minimum. The vertical bars indicate positions at which time measurements were performed, see text.

so to obtain desired phase shift, the time measurements on the magnetized Fe foil with magnetization perpendicular to the $\boldsymbol{E}$ vector of photon were carried out. Results are presented in Fig. 5(a). The results obtained for another direction of magnetization $\boldsymbol{k}$ parallel to $\boldsymbol{E}$) are shown in Fig. 5(b). We see that the spectra shown in Fig. 5, measured at small negative miss-setting Bragg angles (leftmost bar in Fig. 4), are similar to those shown in Fig. 3. Same similarity is observed for large positive miss-setting angles (rightmost bar in Fig. 4): the spectra in the bottom of Figs. 5(a) and (b) are similar to those in Figs. 3(a) and (b). This indicates, as expected, that at large (small) off-Bragg angles, the Si plate does not change the polarization state of photons.

The beam polarization is changed when the Si plate is set close to the Bragg peak. Then, the time spectra, shown in the middle of Fig. 5(a), become similar to those in Fig. 5(b). Simulated spectrum, corresponding to circularly polarized beam and in-plane magnetized foil with already determined parameters (see Fig. 3), is shown in Fig. 6. This spectrum is different

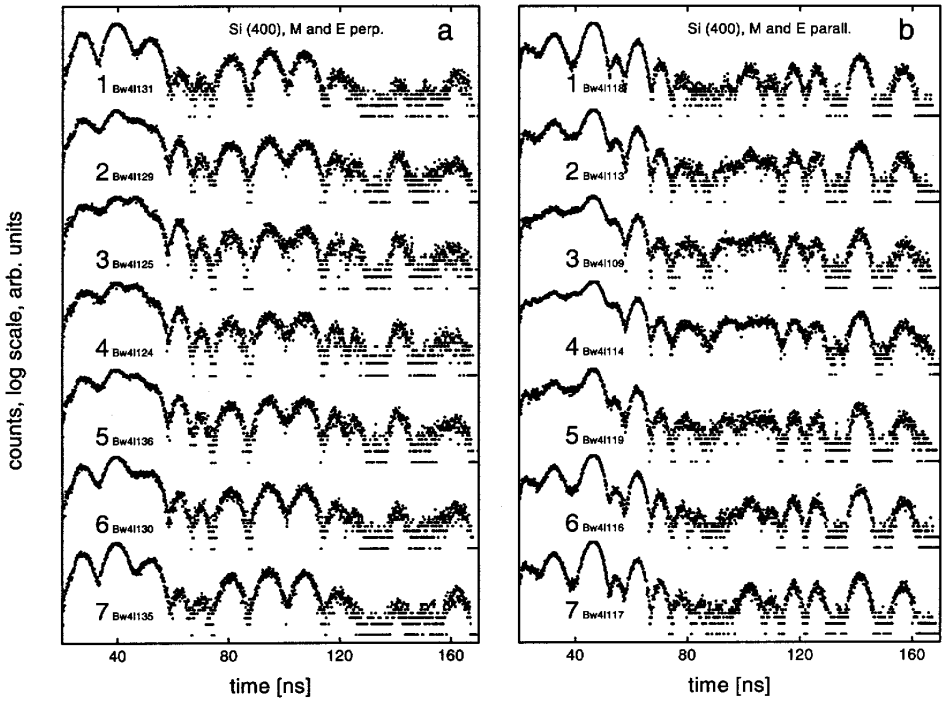


Fig. 5. Rocking curve of the transmitted intensity (Bragg geometry) in the vicinity of Si(4 0 0) Bragg peak. Horizontal scale was set to have 0 at the position of minimum. The vertical bars indicate positions at which time measurements were performed, see text.

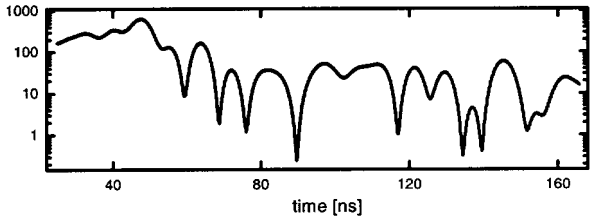


Fig. 6. Simulated NRS spectrum of the ^{57}Fe foil measured with circularly polarized beam.

from the ones presented in Fig. 5. This is due to the fact that the phase shift of photons is distributed in result of the too large angular beam divergence, and well defined polarization state could not be achieved. In order to demonstrate that beam divergence plays crucial role, set of transmission measurements in the vicinity of Si(4 0 0) Bragg peak was performed with

various vertical and horizontal slits sizes. The results, presented in Fig. 7 clearly show that a decrease of the beam divergence affects the angular shape of the transmitted intensity. One can estimate from the uppermost spectrum of Fig. 7 that the FWHM does not exceed 30 μrad and this value is the upper limit of the broadening caused by Si mosaicity, in agreement with our expectation.

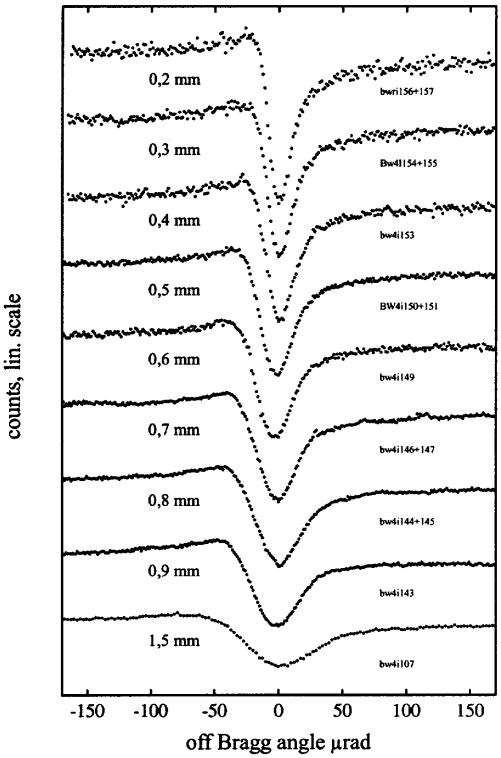


Fig. 7. Rocking curve of the transmitted intensity measured at the same geometry as in Fig. 4. The numbers indicate the slit size. Horizontal scale was set to have 0 at the position of minimum.

4. Discussion

Results of fitting (performed using MOTIF package [17]) theoretical to the two experimental spectra of ^{57}Fe magnetized foil, measured with two linear polarization states of the beam, is shown in Fig. 3. At first trial the only free parameters that depended on the sample, were hyperfine magnetic field $B_{\rm hf}$, and effective thickness τ. We assumed that local magnetization

is perfectly aligned, horizontally (Fig. 3(a)) or vertically (Fig. 3(b)). There are some discrepancies between the experimental and predicted ideal spectra shown by the thin lines in Figs 3(a) and (b), respectively. Next, we assumed that the thickness parameter is nonuniform in the region probed by the beam. Using the Gaussian distribution of the thickness parameter we performed averaging assuming that components corresponding to different thickness add incoherently. The transverse coherence length of the SR in a forward nuclear resonant scattering experiment reported in [18] was about 30 nm. Since in our experiment the beam probe is measuring a few hundreds of μm, the condition for incoherent scattering is obviously fulfilled. Using the Gaussian distribution of the thickness parameter we found better agreement, particularly in the vicinity of the minima corresponding to the dynamical beats (see lines at $t = 70$ and 140 ns in Fig. 3(a), and at $t = 100$ ns in Fig. 3(b)). From the fits we got $B_{\rm hf} = 32.9 \pm 0.1$ T, average effective thickness $\tau = 192 \pm 5$ and the width of the distribution of the effective thickness, $\sigma_\tau = 14$. Assuming the recoilless fraction to be 0.85 and isotopic abundance of ^{57}Fe $90 \pm 5\%$ (this value is not precisely known), one expects to obtain effective thickness ranging between 160 and 230, in good agreement with the value obtained from the fit.

Using the two wave fields approach of dynamical theory [19] we have simulated wave field in the Si plate with parallel surfaces. Rocking curves of the transmitted fields for two linear polarizations are shown in Fig. 8. It is seen, that for large miss-setting angles from the Bragg peak the transmitted intensity is reduced by approximately 50%, while in the vicinity of the Bragg peak, within 10 μrad, all radiation is scattered (only small part absorbed) and no transmitted intensity is present. It follows from Fig. 8(b) that the $\pi/4$ phase difference for σ and π polarization states can be obtained at off-Bragg position of the plate equal to about -13.8 and $+22.5$ μrad.

The measured shape of the rocking curve (Fig. 4) is different from the one predicted by the theory. As it was aforementioned, the difference is due to too high angular beam divergence used in the experiment. Although high resolution Si(4 2 2)×Si(12 2 2) nested monochromator produces a vertical beam divergence of about 20 μrad, horizontal divergence is few times larger. Vector $\boldsymbol{n}$ normal to diffracted planes of our Si crystals was tilted by $\pi/4$ from the x direction (see Fig. 1). The angular divergence of the beam, controlled by pair of slits only, is quite poor. Indeed, for the slits opening and the distance given in paragraph 3, the maximum angular divergence in vertical or horizontal direction amounts to about 170 μrad. This is, however estimation of the upper limit of the angular divergence. To have its better estimation we have performed convolution of the intensity curves presented in Fig. 8(a) with a triangular function of various width. The results are presented in Fig. 9. The obtained shapes can be easily compared with the

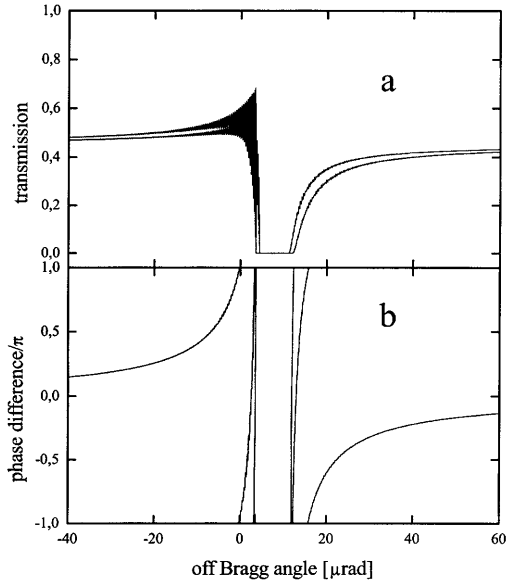


Fig. 8. (a) Simulated rocking curve for Si(4 0 0) transmitted intensity (symmetric Bragg geometry) simulated for 100 μm Si plate. Two lines correspond to σ and π linear polarizations. (b) difference of the phase shift for the transmitted fields with σ and π polarizations.

rocking curves obtained for various slit sizes. For given slit size one can find maximum and minimum of the intensity of the rocking curve, and define the ratio $I_{\min}/I_{\max}$. Then, using convoluted curves in Fig. 9, one can find the width φ of the triangular resolution function which produces identical ratio $I_{\min}/I_{\max}$. Results of the comparison are presented in Fig. 10 by squares. The characteristic width of the rocking curve can also be estimated from the distance between angular positions of the $I_{\min}$ and $I_{\max}$. From the value of this distance one can similarly find the width φ of the triangular resolution function. The results are shown in Fig. 10 by circles. We see that both types of estimation of the width of the resolution function φ agree with each other and indicate proportionality between slit size and the φ. We also notice, that maximal beam divergence, defined by the ratio of the double slit size and the distance between the slits in our experiment, is larger then the required width φ of the resolution function by a factor of 1.3 ± 0.2.

The discussion presented above explains why the measured rocking curve, shown in Fig. 4, is so broad and shallow with respect to the simulated one shown in Fig. 8. The slits used in this experiment correspond roughly to the triangular resolution function with the width of about 120 μrad. We have

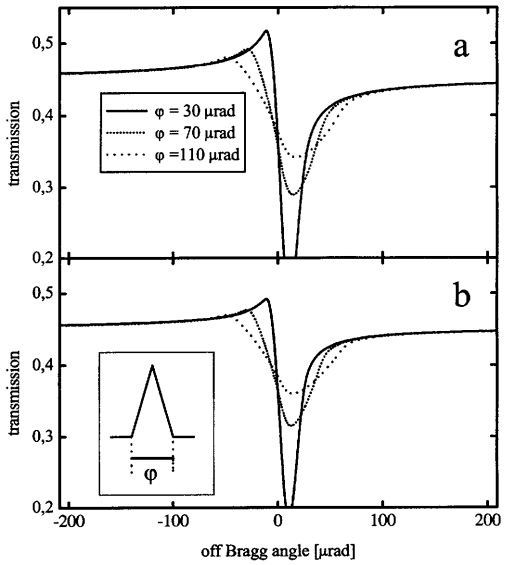


Fig. 9. Convolution of the rocking curve with triangular resolution function (see inset) of different width φ. (a) and (b) correspond to two polarizations indicated in Fig. 8. Note that vertical scales in Figs. 8 and 9 are different.

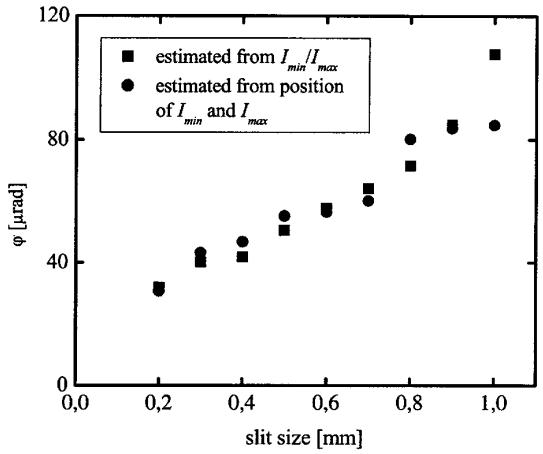


Fig. 10. Estimation of the width φ of the triangular resolution function performed by comparison of the experimental and theoretical relative intensity (squares) and the width (circles).

shown that the decrease of the angular spread of the beam (by varying the slit size) results in narrowing the shape of transmitted intensity. For the smallest slit size, 0.2 mm, at which the intensity was still reasonable, maximum beam divergence had an order of magnitude of the Darwin width. However, very low counting rate prevented us from carrying out time measurements. It is clear that better collimation is required. This can be achieved for example at ID18 or ID22 stations at ESRF, where beam divergence can be reduced below 10 μrad [20]. One can also think about an enhancement of the angular acceptance range when highly asymmetric Bragg geometry is used. Our simulations indicate that for Si(4 0 0) Brag reflection, at incidence above critical angle, equal to 0.002 rad, the Darwin width may increase by an order of magnitude.

Although the used beam station turned out to offer rather unsatisfactory conditions, remarkable change of the shape of time spectra was observed, see middle part of the Fig. 5. Quantitative analysis of the polarization degree is underway. In this report we have demonstrated that cheap and easily available Si plate can be used to obtain circularly polarized resonant radiation. We also presented simple way of checking whether polarization state of the beam was transformed from a linear to the circular one by using the hyperfine structure of ^{57}Fe nucleus.

This work was supported by the IHP-Contract HPRI-CT-2001-00140 of the EC. The authors thanks to D.L. Nagy, L. Bottyan, L. Deak and Y.V. Shvydk'o for valuable discussions, members of the "Hyperfine Interaction" group for technical help, and J. Milczarek for performing neutron check of the crystal quality.

REFERENCES

[1] E. Gerdau, R. Rüffer, R. Hollatz, J.P. Hannon, *Phys. Rev. Lett.* **57**, 1141 (1986).

[2] J.B. Hastings, D.P. Siddons, U. van Bürck, R. Hollatz, U. Bergmann, *Phys. Rev. Lett.* **66**, 770 (1991).

[3] E. Gerdau, U. van Bürck, in: *Resonant Anomalous X-ray Scattering, Theory and Applications*, eds. G. Materlik, C.J. Sparks, K. Fischer, North-Holland, Amsterdam 1994, p. 589.

[4] R. Rüffer, H.D. Rüter, E. Gerdau, *Hyp. Int.* **123/124**, 405 (1999).

[5] Y.V. Shvyd'ko, *Hyp. Int.* **123/124**, 275 (1999).

[6] H. Frauenfelder, D.E. Nagle, R.D. Taylor, D.R.F. Cochran, W.M. Visscher, *Phys. Rev.* **126**, 1065 (1962).

[7] K. Hirano, K. Izumi, T. Ishikawa, S. Annaka, S. Kikuta, *Jpn. J. Appl. Phys.* **30**, L407 (1991).

[8] T. Ishikawa, K. Hirano, S. Kikuta, *J. Appl. Cryst.* **24**, 982 (1991)

[9] C. Giles, C. Malgrange, J. Goulon, F. de Bergevin, C. Vettier, A. Fontaine, E. Dartyge, S. Pizzini, *Nucl. Instrum. Methods Phys. Res.* **A349**, 622 (1994).

[10] A. Kaprolat, K.-J. Gabriel, W. Schülke, P. Fischer, G. Schütz, *Nucl. Instrum. Methods Phys. Res.* **A361**, 358 (1995).

[11] O. Leupold, J. Pollmann, E. Gerdau, H.D. Rüter, G. Faigel, M. Tegze, G. Bortel, R. Rüffer, A.I. Chumakov, A.Q.R. Baron, *Eruphys. Lett.* **35**, 671 (1996).

[12] C.L. L'Abbé *et al.* APS Activity Report, ANL-02/06 December (2002).

[13] V.A. Belyakov, V.E. Dmitrenko, *Sov. Phys. Usp.* **32**, 697 (1989).

[14] G.V. Smirnov, *Hyp. Int.* **123/124**, 31 (1999).

[15] U. van Bürck *Hyp. Int.* **123/124**, 483 (1999).

[16] Yu. Shvyd'ko, Experience at Hasylab F4; October 1994/May (1995).

[17] Yu. Shvyd'ko, *Hyp. Int.* **125**, 173 (2000).

[18] A.Q.R. Baron *et al.*, *Phys. Rev. Lett.* **77**, 4808 (1996).

[19] A. Authier, *Dynamical Theory of X-Ray Diffraction*, Oxford University Press, Oxford 2001.

[20] O. Leupold, private information, also: www.esrf.fr/Accelerators/Performance